Numerical Simulation of Two-Dimensional Freejet Flow-Fields

By

Koji TESHIMA* and Hiroyuki NAKATSUJI*

(January 27, 1986)

Summary: Supersonic jet flow-fields from a two-dimensional sonic nozzle are computed using the piecewise linear method. The sonic radius for a two-dimensional source flow is estimated using the numerical results. It is shown that the flow properties on the jet axis can be approximated by the two-dimensional source flow at large distances from the nozzle. The distance of the normal shock from the nozzle increases with the stagnation to ambient pressure ratio, but is somewhat larger than experiments.

§I. INTRODUCTION

Supersonic jets from two-dimensional sonic nozzles are applicable in many engineering purposes, such as mass separation and producing high energy neutral beams. In the present paper numerical simulations are made for two-dimensional freejets of an inviscid, non-heatconducting, compressible gas using the piecewise linear method (PLM) [*1*], which has been shown to be an appropriate scheme for flows accompanying with shocks [*2*]. The results are compared with a two-dimensional source flow expansion and with the existing experimental data [*3–5*].

§II. METHOD OF CALCULATION

The basic equations of continuity, momentum and energy for two-dimensional, non-heatconducting, non-stationary, inviscid, compressible gas flows, written in the vector form, are given as

$$\frac{\partial \boldsymbol{U}}{\partial t}+\frac{\partial \boldsymbol{F}}{\partial x}+\frac{\partial \boldsymbol{G}}{\partial y}=0 \tag{1}$$

where

$$\boldsymbol{U}=\begin{pmatrix}\rho\\ \rho u\\ \rho v\\ \rho e\end{pmatrix},\qquad \boldsymbol{F}=\begin{pmatrix}\rho u\\ \rho u^2+p\\ \rho uv\\ \rho u(e+p/\rho)\end{pmatrix},\qquad \boldsymbol{G}=\begin{pmatrix}\rho v\\ \rho uv\\ \rho v^2+p\\ \rho v(e+p/\rho)\end{pmatrix} \tag{2}$$

and x, y, t, p, ρ, e, u and v denote the two spatial coordinates ($x=0$ at the nozzle exit and $y=0$ at the center of the nozzle), time, static pressure, density, total energy per unit

* Department of Aeronautical Engineering, Kyoto University.

mass, x- and y-components of flow velocity, respectively. The total energy ,e, is the sum of both the internal and the kinetic energies, and is expressed for a perfect gas as

$$e=\frac{p/\rho}{\gamma-1}+\frac{1}{2}(u^2+v^2) \tag{3}$$

where γ is the ratio of specific heats.

In the present study, the governing equations, eq. (1), are solved by using the time-splitting method. Namely, the basic equations are approximated by the following two sets of equations and the solutions at each time step are obtained by solving them successively.

$$\frac{\partial \boldsymbol{U}}{\partial t}+\frac{\partial \boldsymbol{F}}{\partial x}=0, \qquad \frac{\partial \boldsymbol{U}}{\partial t}+\frac{\partial \boldsymbol{G}}{\partial y}=0 \tag{4}$$

The three equations of the first (second) set of equations in eq. (4) form the basic equations of one-dimensional flow in the x (y) direction. The remaining equation of each set is the transport equation of the momentum in the transverse direction. A one-dimensional Eulerian version of the PLM is used to solve the former, and then the latter is solved with a time-forward space-centered finite difference scheme. The time step is forwarded until a steady solution is obtained under appropriate boundary conditions. The details of the scheme for the PLM are given in the literatures [*1, 2, 6–8*].

Figure 1 shows the grid points used in the present calculations. NX and NY equally spaced grid points are used in the both directions. Up to 240 for NX and 180 for NY, were taken depending on the value of the stagnation to the ambient pressure ratio, p_0/p_∞ and four grid points were assigned to the width of the nozzle exit. Sonic conditions were applied to the nozzle exit while mirror reflections were assumed on the solid wall of the left boundary. At the circumference, namely at the top of Fig. 1, the ambient conditions ($p=p_\infty$, $\rho=\rho_\infty$, $u=v=0$) were used as the boundary conditions. The conditions of zero-gradients of flow parameters, flow-out conditions, were used at the right-hand side of the calculation region. Sonic conditions were distributed initially to the shaded area in Fig. 1. The ambient conditions were given to the rest of the grid points as the initial conditions. The value of time increment was determined at each time step considering the CFL stability condition.

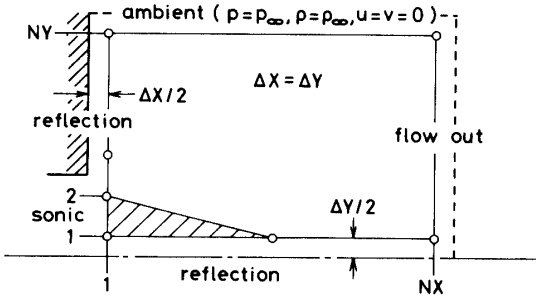

Fig. 1. Calculation region and initial and boundary conditions.

§III. Numerical Results

Calculation was made for a gas with $\gamma=1.4$ and for the pressure ratios, 10, 20, 30, 40 and 50. The stagnation temperature, T_0, and the ambient gas temperature, T_∞, were assumed to be the same. Steady solutions were obtained for the flow-fields upstream of the normal shock within time steps of 800 to 2000 depending on the values of the pressure ratio.

Isobars, velocity vectors in the flow fields and profiles of the density and velocity along the jet axis are shown in Fig. 2 for $p_0/p_\infty=50$. The location of the normal shock is seen as a sharp jump in the figure and neither undershoot nor overshoot is observed across it.

§IV. Comparison With A Two-Dimensional Source Flow And With Experiments

For a two-dimensional source flow, the continuity equation can be written as

$$\rho u r=\rho^* u^* r^* \tag{5}$$

where r is the radial distance from the source and the asterisk denotes the sonic condition. Using the isentropic relations, density reduced by its source value, ρ_0, can be written as

$$\frac{\rho}{\rho_0}=\beta\left(\frac{2}{\gamma+1}\right)^{1/(\gamma-1)}\left(\frac{\gamma-1}{\gamma+1}\right)^{1/2}\left(1-\frac{T}{T_0}\right)^{-1/2}\left(\frac{x}{D}\right)^{-1} \tag{6}$$

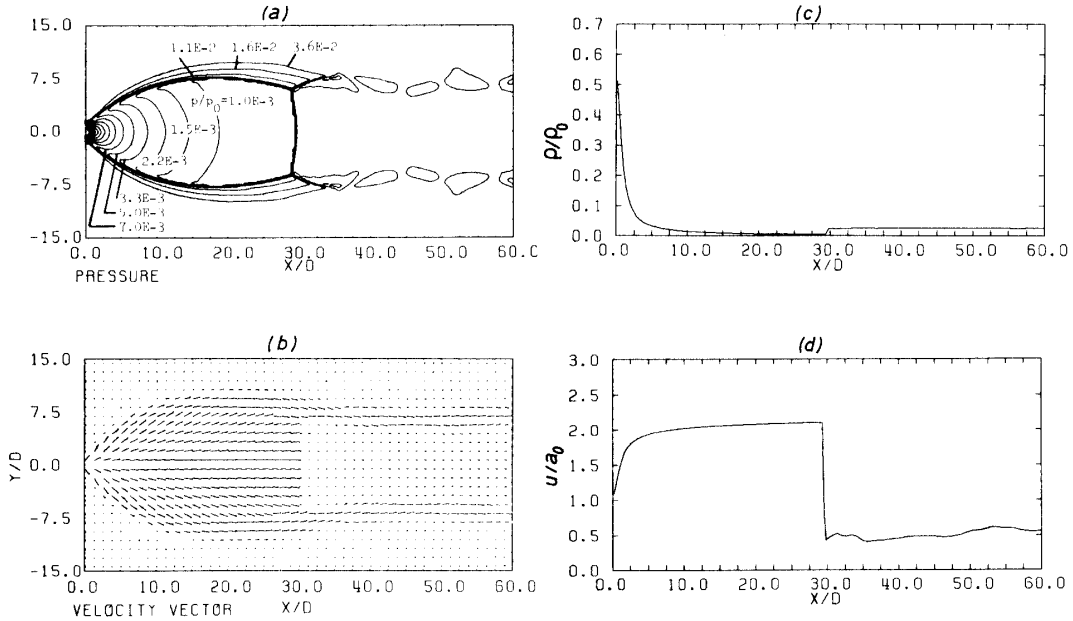

Fig. 2. Numerical results for $p_0/p_\infty=50$: (a) Isobars, (b) Velocity vectors, (c) Density profile on jet axis, (d) Velocity profile on jet axis.

Here, in order to express the density as a function of the distance x measured by the width, D, of the nozzle, we have made that $r=x$ and $r^*=\beta D$. Using the calculated values of density and temperature on the jet axis one can calculate the value of β, which is shown in Fig. 3 as a function of x/D. It can be seen for large values of x/D (>7.5) it converges to a value, which is close to 0.5. Therefore, for such large x/D the flow properties of the two-dimensional freejet on axis can be approximated well by a two-dimensional source flow with a sonic radius of about a half of the nozzle width.

The value of β can be deduced also from the density distribution in y direction [9]. The radial density distribution in an axisymmetric freejet can be approximated well by the Boynton's formula [10],

$$\frac{\rho(r,\theta)}{\rho(r,0)}=\cos^{2/(\gamma-1)}\left(\frac{\pi}{2}\frac{\theta}{\theta_m}\right), \qquad \theta_m=\frac{\pi}{2}\left(\sqrt{\frac{\gamma+1}{\gamma-1}}-1\right) \tag{7}$$

where $\rho\ (r,\ \theta)$ is the density at r and angle θ measured from the jet axis. This has been confirmed using the numerical results of the axisymmetric freejet using the same

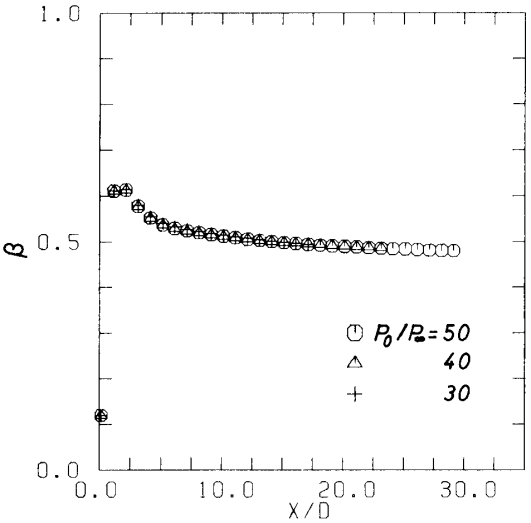

Fig. 3. Value of β as a function of x/D.

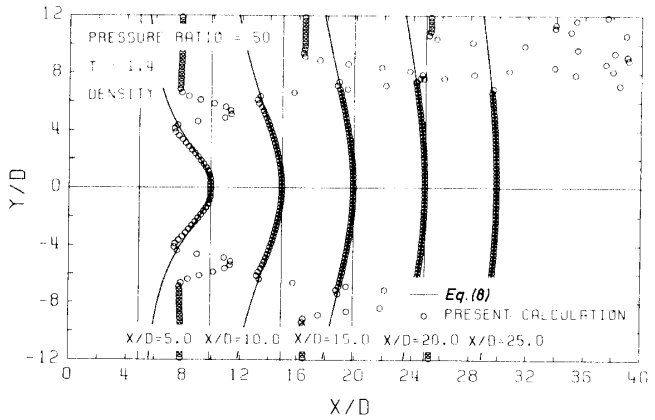

Fig. 4. Comparison of calculated density distributions in y direction with empirical formula, eq. [8].

numerical method as the present one.

From a simple consideration the exponent of cosine in eq. [7] will be $1/(\gamma-1)$ for the two-dimensional case. Then the density distribution in y direction can be written as

$$\frac{\rho(x, y)}{\rho(x, 0)}=\cos\theta\cos^{1/(\gamma-1)}\left(\frac{\pi}{2}\frac{\theta}{\theta_m}\right) \tag{8}$$

Eq. [8] is compared with the numerical results in Fig. 4. Again for large values of x/D they agree very well. The integrated flow rate with respect to θ from 0 to θ_m must be equal to that for a nozzle of width D. Then using eq. [5], β can be written as

$$\beta=\left[2\int_0^{\theta_m}\cos^{1/(\gamma-1)}\left(\frac{\pi}{2}\frac{\theta}{\theta_m}\right)d\theta\right]^{-1} \tag{9}$$

For $\gamma=1.4$ the value of β becomes 0.481, which is close to the value previously obtained.

The Mach number, M, on the jet axis can be approximated from eq. [6] using the relation, $T/T_0=[1+(\gamma-1)M^2/2]^{-1}$, as

$$M\cong B\left(\frac{x}{D}\right)^{(\gamma-1)/2}-\frac{1}{2}\left(\frac{\gamma+1}{\gamma-1}\right)\Big/B\left(\frac{x}{D}\right)^{(\gamma-1)/2}, \quad B=\beta^{-(\gamma-1)/2}\left(\frac{\gamma+1}{\gamma-1}\right)^{(\gamma+1)/4}, \tag{10}$$

which is similar to the expression for the axisymmetric jet [11], in which the dependence of x/D is $(x/D)^{\gamma-1}$. Using the value $\beta=0.5$ the Mach number distribution can be approximated well with eq. [10] as shown in Fig. 5.

The location of the normal shock on the axis measured with D, x_M/D' can be estimated from eq. [10] using the normal shock relation as

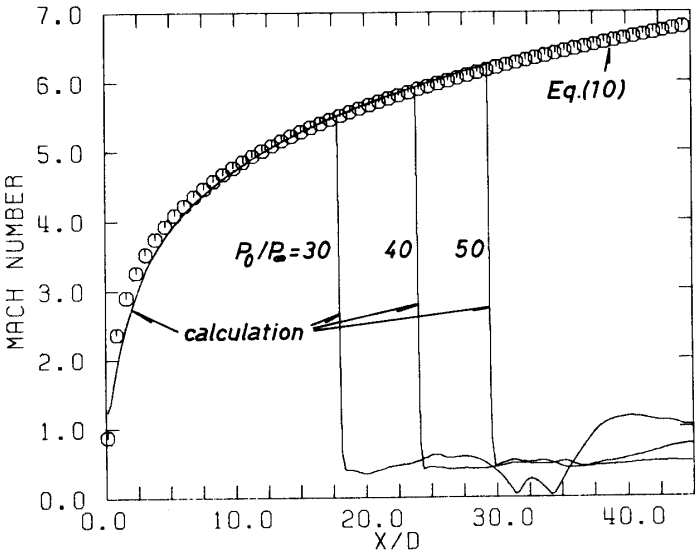

Fig. 5. Mach number change along jet axis.

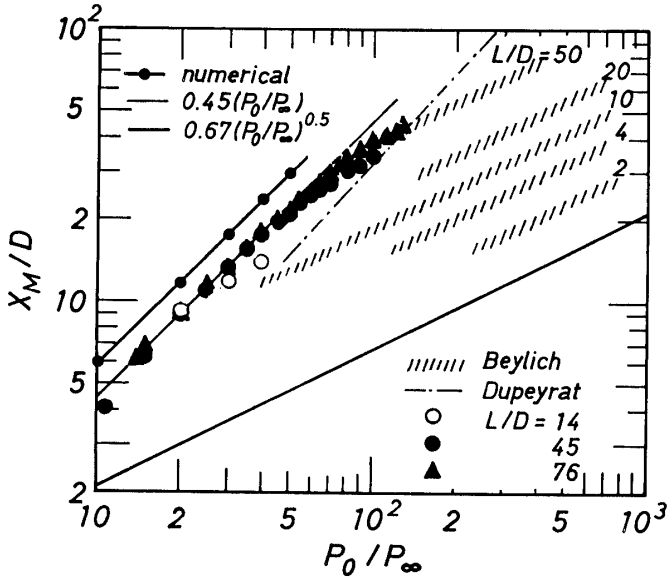

Fig. 6. Reduced normal shock location as a function of pressure ratio: Comparison of calculation with experiments.

$$\frac{x_M}{D}=C\left(\frac{p_0}{p_\infty}\right), \tag{11}$$

where C is a constant including the values of β and γ. For $\beta=0.5$, C=0.75, while the numerical results give C=0.59.

Some experiments have been made for freejets from slit nozzles with finite aspect ratios, L/D, (L being the length of the slit). Beylich [3] measured the normal shock position for slits with small aspect ratios and have shown that for large pressure ratios, it increases with the square root of the pressure ratio, same as for the axisymmetric jet, but expected that for smaller values of the pressure ratio it increases linearly. He expected $C=A^2$, where A is the proportionality constant in the expression of the Mach disk location for the axisymmetric jet [11]. Dupeyrat [4] used large aspect-ratio slits at much larger pressure ratios, and showed that almost linear dependence of x_M on the pressure ratio, but gave a smaller value of C. We recently measured x_M for slits with several different aspect ratios at smaller pressure ratios, where the Beylich's experiment has not covered [5], using the laser induced fluorescence method [12]. As is shown in Fig. 6, x_M increases linearly with the pressure ratio until a certain value, depending on the aspect ratio and then seems to follow the same pressure dependence as for the axisymmetric jet. This experimental result gives C=0.45. Since A=0.67 [11], then this value of C agrees well with the value expected by Beylich. But the present numerical result gives about 1.3 times larger than these values. Two possible reasons for this are 1) the number of grid points for the nozzle exit was four in the present calculation and this may not be enough to express the width of the nozzle correctly, and 2) three dimensionality in the shapes of the jets issuing from a slit with a finite aspect ratio may shorten the distance at which the normal shock occurs. Further numerical and experimental studies are now in progress.

§V. Conclusions

Supersonic jet flow-fields from a two-dimensional sonic nozzle are computed using the piecewise linear method. The sonic radius for the two-dimensional source flow was estimated using the numerical results. The flow properties on the jet axis are approximated well by the two-dimensional source flow with a sonic orifice of about a half of the nozzle width at large distances from the nozzle ($x/D>7.5$). Dependence of the location of the normal shock on the pressure ratio is linear but somewhat larger than experiments.

§V. Acknowledgements

The present work was partially supported by the Data Processing Center of Kyoto University as one of its Program Development Projects.

References

[1] Woodward, P. R. and Colella, P.: High Resolution Difference Schemes for Compressible Gas Dynamics, Lecture Notes in Physics, *141* (1981) pp. 434–441.

[2] Saito, S., Nakatsuji, H. and Teshima, K.: Numerical Simulation and Visualization of Freejet Flow-Fields, Transactions of Japan Soc. for Aeron. and Space Sci. *28* (1986) pp. 240–247.

[3] Beylich, A. E.: Struktur von Überschall-Freistrahlen aus Schlitzblenden, Z. Flugwiss. Weltraumforsch. *3* (1979), Heft 1, pp. 48–58.

[4] Dupeyrat, G.: Two- and Three-Dimensional Aspects of a Freejet issuing from a Long Rectangular Slit, Rarefied Gas Dynamics, S. S. Fisher Ed., AIAA Press, New York, 1981, pp. 812–819.

[5] Teshima, K. and Nakatsuji, H.: Numerical and Experimental Studies of Two-Dimensional Freejets and Their Interactions, (unpublished).

[6] Woodward, P. R. and Colella, P.: The Numerical Simulation of Two-Dimensional Fluid Flow with Strong Shocks, J. Comp. Phys., *54* (1984) pp. 115–173.

[7] Colella, P., and Glaz, H.: Efficient Solution Algorithms for the Riemann Problem for Real Gases, Lawrence Berkeley Laboratory Report LBL-15776, 1983.

[8] van Leer, B.: Towards the Ultimate Conservative Difference Scheme. V. A. Second-Order Sequel to Godunov's Method, J. Comp. Phys., *32* (1979) pp. 101–136.

[9] Mikami, H.: Transport Phenomena in Free-Jet Expansions, Bull. Res. Lab. for Nucl. Reactors. *7* (1982) pp. 151–187.

[10] Boynton, F. P.: Highly Underexpanded Jet Structure: Exact and Approximate Calculations, AIAA J., *5* (1967) pp. 1703–1704.

[11] Ashkenas, H., and Sherman, F. S.: The Structure and Utilization of Supersonic Free Jets in Low Density Wind Tunnels, Rarefied Gas Dynamics, J. H. deLeeuw, Ed., Academic Press, New York, 1966, vol. II, pp. 84–105.

[12] Teshima, K., Moriya, T., and Mori, T.: Visualization of a Free Jet by a Laser Induced Fluorescence Method, J. Japan Soc. Aero. and Space Sciences, *32* (1984) pp. 61–64. (in Japanese): Teshima, K. and Nakatsuji, H.; Viaualization of Rarefied Gas Flows by a Laser Induced Fluorescence Method, Rarefied Gas Dynamics, H. Oguchi, Ed., University of Tokyo Press, 1984, pp. 447–454.